Journal of Molecular Liquids 434 (2025) 128069

Contents lists available at ScienceDirect

Journal of Molecular Liquids

journal homepage: www.elsevier.com/locate/molliq

Role of electrolytes and co-surfactants on the rheological properties of sodium N-acyl sarcosinate solutions

Dilek Gazolu-Rusanova [a,b], Marina Stoeva [a], Zlatina Mitrinova [a], Nevena Pagureva [a], Nikola Burdzhiev [c], Slavka Tcholakova [a,*]

[a] Department of Chemical and Pharmaceutical Engineering, Faculty of Chemistry and Pharmacy, Sofia University, 1164 Sofia, Bulgaria
[b] Centre of Competence "Sustainable Utilization of Bio-resources and Waste of Medicinal and Aromatic Plants for Innovative Bioactive Products" (BIORESOURCES BG), Sofia, Bulgaria
[c] Department of Organic Chemistry and Pharmacognosy, Faculty of Chemistry and Pharmacy, Sofia University, 1164, Sofia, Bulgaria

ARTICLE INFO

Keywords:
Sodium N-acyl sarcosinate
Salt curves
Phase behaviour
Micellar growth

ABSTRACT

Alkyl sarcosinates are amino acid-based anionic surfactants commonly used as primary surfactants in sulfate-free personal care products. The major aim of this study is to identify the key factors influencing the rheological behaviour of sodium sarcosinate solutions and their mixtures with nonionic, zwitterionic, and cationic co-surfactants. To achieve this, we examined the effects of salt type and concentration for alkyl sarosinates with different chain lengths (dodecyl, tetradecyl, and cocoyl) across concentration range of 2–20 wt%. Experimental results reveal two distinct regions in the salt curve for the three studied sarcosinates. At low electrolyte concentrations, viscosity remains constant until reaching the critical electrolyte concentration, C_1, beyond which viscosity increases logarithmically with salt concentration. Further electrolyte addition leads to phase separated solutions at the critical precipitation concentration, C_{TR}. Both C_1 and C_{TR} decrease as the hydrocarbon chain length increases from dodecyl to tetradecyl. However, the presence of shorter chain molecules in cocoyl sarcosinate significantly increases both C_1 and C_{TR} due to the formation of spherical micelles. A theoretical expression for predicting viscosity dependence on salt concentration is derived and successfully applied to describe the experimental data. The adsorption energy of sodium and potassium to alkyl sacrosinate micelle surfaces is found to be much smaller than that to sodium lauroyl ether sulfate surfactants (1 vs. 3 k_BT for Na^+ and 0.8 vs. 3.8 k_BT for K^+). No significant effect of amphoteric co-surfactants, including cocoamidopropyl betaine, sulfobetaine, or decylamine oxide, is observed. NMR analysis confirms that cocoamidopropyl betaine and sodium dodecyl sarcosinate form mixed micelles that are structurally similar to sarcosinate micelles, as carboxyl groups remain exposed on the micelle surfaces in both cases. When using amine oxide and sulfobetaine, the increase in viscosity is attributed to the elongation of mixed micelles, though steric hindrance from side methyl groups limits their growth. The practical significance of this study lies in the finding that longer-chain alkyl sarcosinates (such as tetradecyl, as investigated here) can attain significantly higher viscosities at lower salt concentrations

Abbreviations and symbols: C_1, limiting salt concentration for micelle growth; C_{TR}, critical salt concentration for precipitation; k_B, Boltzmann constant; T, temperature; SLES, sodium lauryl ether sulfate; CAPB, cocoamidopropyl betaine; Z, counterion charge; R, counterion radius; NaCl, sodium chloride; CAHS, cocoamidopropyl hydroxysultaine; pKa, negative base-10 logarithm of the acid dissociation constant; LiCl, lithium chloride; CTAC, cetyltrimethylammonium chloride; C12P, N-dodecylpyrrolidone; KCl, potassium chloride; NaC_{12}Sarc, sodium N-lauroyl sarcosinate; NaC_{14}Sarc, sodium N-myristoyl sarcosinate; NaCocoylSarc, sodium N-cocoyl sarcosinate; Ammonyx, decylamine oxide; SulfoBetaine, N-dodecyl-*N*,*N*-dimethyl-3-ammonio-1-propanesulfonate; C10TAB, decyltrimethylammonium bromide; DTAB, dodecyltrimethylammonium bromide; CTAB, cetyltrimethylammonium bromide; CMEA, cocamide monoethanolamine; C8Alc, 1-octanol; C8Ac, 1-octanoic acid; SAXS/WAXS, small/wide angle X-ray scattering; NMR, nuclear magnetic resonance; C_S, molality concentration of surfactant; C_{NaCl}, molality concentration of NaCl; p, packing parameter; v, effective molecular volume; l, surfactant length; α_1, fraction of ionized molecules; a_{Sar-}, area per molecule of ionized sarcosinate molecules; a_{MSar}, area per molecule of non-ionized sarcosinate molecules; C_{NaSar}, molality of neutralized NaC_{12}Sarc molecules; C_{Sar-}, molality of ionized sarcosinate molecules; C_{Na+}, molality of free Na^+ not bound to sarcosinate molecules; η, apparent viscosity; K_1, dissociation constant of NaC_{12}Sarc; C_{KSar}, molality of neutralized sarcosinate molecules by K^+; C_{KCl}, molality concentration of KCl; K_2, dissociation constant of potassium sarcosinate; KSarcosinate, potassium sarcosinate; SLD, scattering length density; Rx, Ry, micelle axial dimensions; D, diffusion coefficient; R_H, hydrodynamic radius.

* Corresponding author at: Department of Chemical and Pharmaceutical Engineering, Faculty of Chemistry and Pharmacy, Sofia University, 1 James Bourchier Ave., 1164 Sofia, Bulgaria.
E-mail address: SC@LCPE.UNI-SOFIA.BG (S. Tcholakova).

https://doi.org/10.1016/j.molliq.2025.128069
Received 17 April 2025; Received in revised form 12 June 2025; Accepted 26 June 2025
Available online 28 June 2025

compared to shorter-chain analogs or surfactant mixtures. The scientific significance stems from the development of a theoretical model capable of predicting the viscosity of alkyl sarcosinate solutions across various surfactant and salt concentrations.

1. Introduction

The rheological properties of micellar solutions and viscosity control mechanisms are essential for formulating cosmetic and personal care products. The viscosity of ionic surfactant solutions can be controlled by adding salt and/or combining it with an appropriate co-surfactant. These mechanisms for controlling rheological behaviour have been widely studied and reported for anionic surfactants [1–3], cationic surfactants [4,5] and mixtures of surfactants [6–11].

The viscosity of the ionic surfactant solutions reaches a maximum with an increase in the added salt concentration, represented by salt curves [3,10,11]. The addition of salt leads to a decrease in the electrostatic repulsion between the charged heads of the surfactant molecules [12], which favours micellar growth and transformation of spherical micelles into rod-like or worm-like micelles. The entanglement of worm-like micelles increases bulk viscosity [13]. Upon further increase in electrolyte concentration, entangled micelles can become branched [14–17] or transition to disk-like ones [9]. In both cases, the result is a decrease in viscosity.

The effectiveness of electrolytes to induce micellar growth in a given surfactant system depends on its charge and size. A number of papers discuss the specific interactions that exist between ions and charged headgroups in terms of a Hofmeister type ordering [18–23]. In general, smaller ions with higher charge have higher charge density, making them water-structuring kosmotropes. These ions have larger hydration shells and, therefore, larger effective hydrated radii. As a result, their charge density decreases, which weakens their interactions with oppositely charged ions in water, including those in surfactant systems. According to the model of "matching water affinities" proposed by Collins et al. [24], ions with similar water affinity interact strongly, i.e. small and hard cations interact preferentially with small and hard anions (kosmotropes) and big and "soft" cations with big and "soft" anions (chaotropes) [3,10,18–24]. Pleines et al. [3] show that the position and amplitude of the salt curve of sodium lauryl ether sulfate (SLES) depend on the radius of the hydrated counterion and its charge. A shift of the viscosity peak to lower electrolyte concentrations and a decrease in viscosity at the maximum of the salt curve are observed when using counterions with a smaller radius of the hydrated ion ("soft" cations) such as K^+, which interact more strongly with the SLES molecules ("soft" anion) compared to "hard" cations such as Li^+ [3,21]. The addition of suitable co-surfactants can also influence the rheological behaviour of surfactant solutions [10,11,23]. Mitrinova et al. [10] demonstrate that the addition of cocoamidopropyl betaine (CAPB) to SLES not only results in a higher viscosity of the micellar solution but also significantly affects the interaction between the anionic surfactant and various counterions. The viscosity at the peak of the SLES+CAPB salt curves decreases with increasing radius of the hydrated counterion, which is opposite to the results of Pleines et al. [3] for solutions of SLES alone, without co-surfactant. The electrolyte concentration leading to the maximum viscosity of SLES+CAPB solutions decreases with increasing counterion charge density.

Alkyl sarcosinates are natural anionic surfactants derived from fatty acids and the amino acid sarcosine. This class of surfactants has excellent adsorption and foaming properties, low toxicity, high biodegradability, broad biological activity and mildness to the skin [25–27]. Sarcosinates are used as substitutes for sulfate-containing surfactants (e.g., SLES) in various cosmetic and personal care products, including shampoos, conditioners, shaving and washing products. Sarcosinates exist in equilibrium with small amounts of free N-acyl sarcosine acid in the pH range of 4–7, and the acid is completely solubilised within the micelles in aqueous solution [28].

The viscosity control mechanisms applied to micellar solutions of conventional anionic surfactants (addition of salt and/or amphoteric co-surfactants) have been found to yield insufficient results for most bio-based surfactants. Vu et al. [13] compared the effect of sodium chloride (NaCl) on the viscosity of sodium lauroyl sarcosinate and SLES solutions and found that the viscosity of a sarcosinate solution could not be effectively increased by adding an appropriate amount of salt. The viscosity of SLES solutions reaches a maximum as the NaCl concentration increases. On the other hand, there is no significant change in the viscosity of sodium lauroyl sarcosinate solutions at low NaCl concentrations and a slight increase is observed only at salt concentrations above 16 % wt/v. The lack of thickening effect of NaCl addition is usually attributed to the presence of a methyl group on the amide nitrogen, which leads to a relatively large headgroup area of sodium lauroyl sarcosinate and steric hindrance, preventing the molecules from packing tightly [29,30]. Ray et al. [31] show that monovalent ions binding to the sodium lauroyl sarcosinate head group obey the Hoffmeister series, i.e., the degree of counterion binding increases in the order $Li^+ > Na^+ > K^+ > Cs^+$. However, the packing parameter remains less than 1/3 for all studied counterions, indicating that the micelles have a spherical shape.

Most studies in the literature focus on using co-surfactants and changing pH as alternative thickening tools for sodium lauryl sarcosinate solutions. Varade and Bahadur [32] observe a significant decrease in the critical micelle concentration and an increase in viscosity when mixing 10 mM sodium N-myristoyl sarcosinate with cationic surfactants in varying ratios. Other authors use pH as a parameter to control the viscosity of sodium lauroyl sarcosinate solutions in the presence of amphoteric or nonionic co-surfactants. Lu et al. [33] investigate the rheological behaviour of CAPB/sodium lauroyl sarcosinate systems at different surfactant ratios and as a function of pH. The viscosity of micellar solutions of CAPB/sarcosinate with appropriate mass ratios (4:8–9:3) increases to maximum values and then decreases as the pH of the solution is changed between 4 and 6. The highest viscosity measured is approximately 5.5 Pa.s at a mass ratio of CAPB/sarcosinate of 8:4 and pH = 5.1. Cryo-TEM images reveal the growth of micelles in this system, which is responsible for the peak in viscosity. Upon lowering the pH, CAPB becomes positively charged and exhibits properties of a cationic surfactant, interacting more strongly with the anionic sarcosinate molecules. The authors suggest that this favours the formation of worm-like micelles at an optimal pH and ratio between the two types of surfactants. Vu et al. [13] investigate the effect of pH on the viscosity of the solutions of sodium lauroyl sarcosinate with amphoteric cocoamidopropyl hydroxysultaine (CAHS). The viscosity peak of each system is observed in the pH range of 4.8–5.0, which is close to the experimentally determined pKa of the investigated system. The synergistic effect is strongest at a 6 % sarcosinate +9 % CAHS (equivalent molar ratio 1:1), where the maximum viscosity is 9.6 Pa.s at pH = 4.8. The intermolecular interactions between lauroyl sarcosine acid, anionic sodium lauroyl sarcosinate and CAHS reduce the electrostatic repulsion between molecules, favouring the formation of worm-like micelles and the increase in the viscosity of the formulations. In their following article, Vu et al. [30] study the effect of pH on the thickening of their model formulation of 6 % sarcosinate +9 %CAHS in the presence of various additives such as lithium chloride (LiCl), sodium chloride, L-arginine, triethanolamine, trimethylphenylammonium chloride, and cetyltrimethylammonium chloride (CTAC). The cationic surfactant, CTAC, has the greatest thickening effect and shifts the viscosity maximum to higher pH values. LiCl and NaCl only thicken the formulation at high concentrations (10 %). All other tested additives are ineffective or

inefficient at thickening the sarcosinate/CAHS mixture.

Varade et al. [34] also show that adjusting the pH close to pKa significantly increases the viscosity of the mixture of sodium lauroyl sarcosinate with the nonionic cocamide monoethanolamine and lauryl glucoside. Liu et al. [35] achieve viscosity enhancement in the aqueous solution of sodium lauroyl sarcosinate by adding N-dodecylpyrrolidone (C12P), a nonionic surfactant with a relatively small headgroup. The maximum viscosity of the mixed surfactant systems depends on pH, temperature, the concentration of added C12P, and the mass ratio of sodium lauroyl sarcosinate to C12P.

In summary, most studies focus on the effect of various factors on the viscosity control of sodium lauroyl sarcosinate solutions at pH close to pKa. The information on the impact of electrolytes and co-surfactants at neutral or higher pH is scarce. This work aims to determine the effect of the type and concentration of electrolyte (NaCl and KCl) on the phase behaviour and viscosity of sodium N-lauroyl, cocoyl and myristoyl sarcosinate solutions in the presence and absence of different types of co-surfactants in the system at natural pH, which varies between 6.2 and 9.1, where the alkyl sacosinate molecules are ionized. Such a study can expand the knowledge about the properties and phase behaviour of this class of surfactants and be of great importance for the application of this class of surfactants in personal and home care products.

2. Materials and methods

2.1. Materials

Anionic surfactants sodium *N*-lauroyl sarcosinate (NaC_{12}Sarc, 98 % active compound, TCI Chemicals, M_W = 293.38 g/mol), sodium *N*-myristoyl sarcosinate (NaC_{14}Sarc, 30 % active compound, Perlastan M-30 product of Schill+Seilacher, M_W = 321.44 g/mol) and Sodium *N*-cocoyl sarcosinate (NaCocoylSarc, 30 % active compound, Perlastan C-30 product of Schill+Seilacher, M_W = 298.99 g/mol) are used. According to Ref. [36], the cocoyl sarcosinate has the following distribution of the chain lengths: 5.5 % C8, 5.5 % C10, 61.5 % C12, 20.5 % C14, 5 % C16, 2 % C18. The studied zwitterionic co-surfactants are cocamidopropyl betaine (CAPB, TEGO Betaine F50, a product of Goldschmidt GmbH), decylamine oxide (30 % active compound, Ammonyx DO, a product of Stepan Co.) and *N*-dodecyl-*N*,*N*-dimethyl-3-ammonio-1-propanesulfonate (SulfoBetaine, 98 % active compound, Sigma Aldrich). As cationic co-surfactants, the effect of decyltrimethylammonium bromide (C10TAB, 99 % active compound, TCI Chemicals), dodecyltrimethylammonium bromide (DTAB, 98 % active compound, TCI Chemicals) and cetyltrimethylammonium bromide (CTAB, 98 % active compound, TCI Chemicals) is studied. The other studied co-surfactants are cocamide monoethanolamine (CMEA, 100 % active compound, Stepan Co.), 1-octanol (C8Alc, 99 % active compound, TCI Chemicals) and 1-octanoic acid (C8Ac, 99 % active compound, Sigma Aldrich). The ratio between the anionic surfactant and the co-surfactants is 2:1 for all zwitterionic co-surfactants and CMEA, and 10:1 with all cationic co-surfactants, octanol and octanoic acid. The structural formulas of the studied surfactants and cosurfactants are shown in Table S1.

The effect of sodium chloride (NaCl, Honeywell; solubility in water: 6.2 mol/kg at 25 °C [37]) and potassium chloride (KCl, Merck Supelco; solubility: 4.8 mol/kg at 25 °C [38]) on the properties of surfactant solutions is investigated. It should be noted that, according to the information provided by the manufacturer, TEGO Betain F50 contains a certain amount of sodium chloride. 100 mM CAPB is found to contain 118 ± 6 mM NaCl as an additive [39]. The presence of NaCl in CAPB is taken into account when determining the effect of salt concentration on the solution viscosity.

2.2. Solution preparation

Initially, a concentrated aqueous surfactant solution with a total concentration of 20 wt% is prepared. Then, the required amounts of salt and water are added to obtain a solution with the desired concentration of the various components. All components are dissolved at room temperature, except for the CMEA solutions, which are homogenised at 30 °C. Deionised water from a Milli-Q Organex system (Millipore Inc., USA) is used to prepare the solutions. The samples are stored in an incubator at 25 °C, and their properties are examined at least 24 h after preparation. The pH of the solutions is measured using a SI Analytics Lab 845 pH meter (Fisher brand AB200) at room temperature. The pH and viscosity of the concentrated surfactant solutions before the addition of salts are presented in Table S1. Note that all concentrated solutions (20 wt% surfactant) with or without co-surfactants exhibit Newtonian rheological behaviour in the absence of salts. The pH of all solutions is >6, which is above the pKa and ensures the presence of the anionic form of the alkyl sarcosinate molecules.

2.3. Rheological properties

The rheological behaviour of the isotropic solutions is characterised using a Bohlin Gemini rheometer (Malvern Instruments, UK) with a cone and plate configuration. For samples with a low viscosity <0.5 Pa.s, a cone with a diameter of 60 mm and a truncational angle of 2° is used. For samples with a viscosity above 0.5 Pa.s, a cone with a diameter of 40 mm and an angle of 4° is used. The following protocol is used to conduct the experiments: the samples are thermally equilibrated for 3 min at T = 25 °C, then the shear rate is logarithmically increased from 0.02 to 600 s^{-1}. To construct the salt curves (viscosity as a function of electrolyte concentration), we used: (1) the viscosity at 1 s^{-1} for solutions with high salt concentrations, which exhibit non-Newtonian rheological behaviour, or (2) the average viscosity is calculated from measurements performed at shear rates between 10 and 600 s^{-1} for solutions with low electrolyte concentrations, which behave as Newtonian fluids (see Fig. S1).

2.4. SAXS/WAXS measurements

SAXS measurements of the micellar solutions are carried out on an in-house X-ray scattering system (XEUSS 3.0 SAXS/WAXS System, Xenocs, Sassenage, France) with a CuKα X-ray source (λ = 0.154 nm, Xeuss 3.0 UHR Dual source Mo/Cu, Xenocs, Sassenage, France) and Eiger2 4 M detector (Dectris Ltd., Baden Deattwil, Switzerland) with slit collimation. The apparatus is operated at 50 kV and 0.6 mA. The sample to detector distance (SDD) of 1000 mm and 3000 mm allowed to access the Q-range of 0.01–0.5 $Å^{-1}$. The data acquisition time is 20 min. Samples are enclosed in a vacuum-tight thin borosilicate capillary with an outer diameter of 1 mm and a thickness of 10 μm. The scattered intensity is normalised to the incident intensity and is corrected for the background scattering from the capillary. It is calibrated to an absolute scale. The measurements are performed at an ambient temperature of 25 °C. The software SASView is used for modelling SAXS data (http://www.sasview.org).

2.5. NMR measurements

The NMR measurements are carried out on a Bruker Avance III HD 500 MHz spectrometer (Rheinstetten, Germany) fitted with a high-resolution broadband probe-head with Z gradient. The experiments are conducted at T = 25 °C. The studied samples are prepared as described in Section 2.2. 0.5 mL of the sample and 0.1 mL of deuterium oxide (99.8 atom% D) with TMSP-Na-2,2,3,3-d4 as internal standard are mixed before measurement. The Topspin 3.6.5 software package (Bruker) is used for collecting spectra and analysing data.

3. Experimental results and discussion

3.1. Sodium N-lauroyl sarcosinate solutions in presence of NaCl

Sodium lauroyl sarcosinate ($NaC_{12}Sarc$) solutions without added salt exhibit Newtonian rheological behaviour. The viscosity of 10 wt% $NaC_{12}Sarcosinate$ is 2.4 mPa.s, whereas for 20 wt%, it increases to 7.2 mPa.s (see Table S1, Fig. S1). Fig. 1A shows the salt curves for 10 wt% $NaC_{12}Sarc$ solution with added sodium chloride (NaCl). Three distinct regions are observed in the salt curve. At low NaCl concentrations, the viscosity remains relatively constant and close to that of the solution without added electrolyte. When the NaCl concentration exceeds a critical value, denoted as C_1 in Fig. 1A, a sharp increase in viscosity is observed, which continues until the critical concentration for phase separation, C_{TR}, is reached. Beyond this point, the system is no longer isotropic, single-phase or stable, and precipitation occurs, as shown in Fig. S2. The viscosity increase observed between C_1 and C_{TR} is attributed to the formation of elongated micelles.

The determined values of NaCl concentrations corresponding to the onset of viscosity increase, C_1 and of precipitation, C_{TR}, are shown in Fig. 1C as a function of surfactant concentration, C_S. All values are expressed in molality [moles of surfactant or NaCl per kg water]. It is seen that the sum of $C_{TR} + C_S$ remains constant for all studied $NaC_{12}Sarc$ concentrations (ranging from 2 to 20 wt%), indicating that precipitation occurs when molality of Na^+ in the solution exceeds 4.6 mol/kg. The latter confirms that the formed precipitate is sodium lauryl sacrocinate rather than NaCl because the solubility of NaCl in water is 6.2 mol/kg at 25 °C [37]. The obtained C_{TR} for 15 wt% $NaC_{12}Sarc$ is in good agreement with the value reported by Vu et al. [13]. The precipitation of the solutions is attributed to the Krafft point of $NaC_{12}Sarc$. It was found that the Krafft point of 10 wt% $NaC_{12}Sarc$ solution in the presence of 18 wt% NaCl is ~28 °C. Heating the precipitated solutions to 40 °C resulted in the formation of transparent solutions, as shown in Fig. S3.

The NaCl concentration for inducing the viscosity increase, C_1, depends on the C_S by the following expression, see red points in Fig. 1C:

$$C_1 = 1.82C_S^{-0.16} - C_S \quad (1)$$

where C_1 and C_S are expressed in mol/kg water. The above equation allows us to determine the NaCl concentration at which the viscosity increase starts. $NaC_{12}Sarcosinate$ solutions containing NaCl at concentrations below C_1 exhibit Newtonian behaviour, with viscosities increasing almost linearly with surfactant concentration, C_S. This trend is attributed to the increased number concentration of spherical micelles in the solution as C_S increases. In contrast, $NaC_{12}Sarc$ solutions containing NaCl at a concentration above C_1 exhibit non-Newtonian behaviour, see Fig. S1. In these systems, the dependence of viscosity on shear rate, $\eta(\dot{\gamma})$, consists of two well-defined regions: at low shear

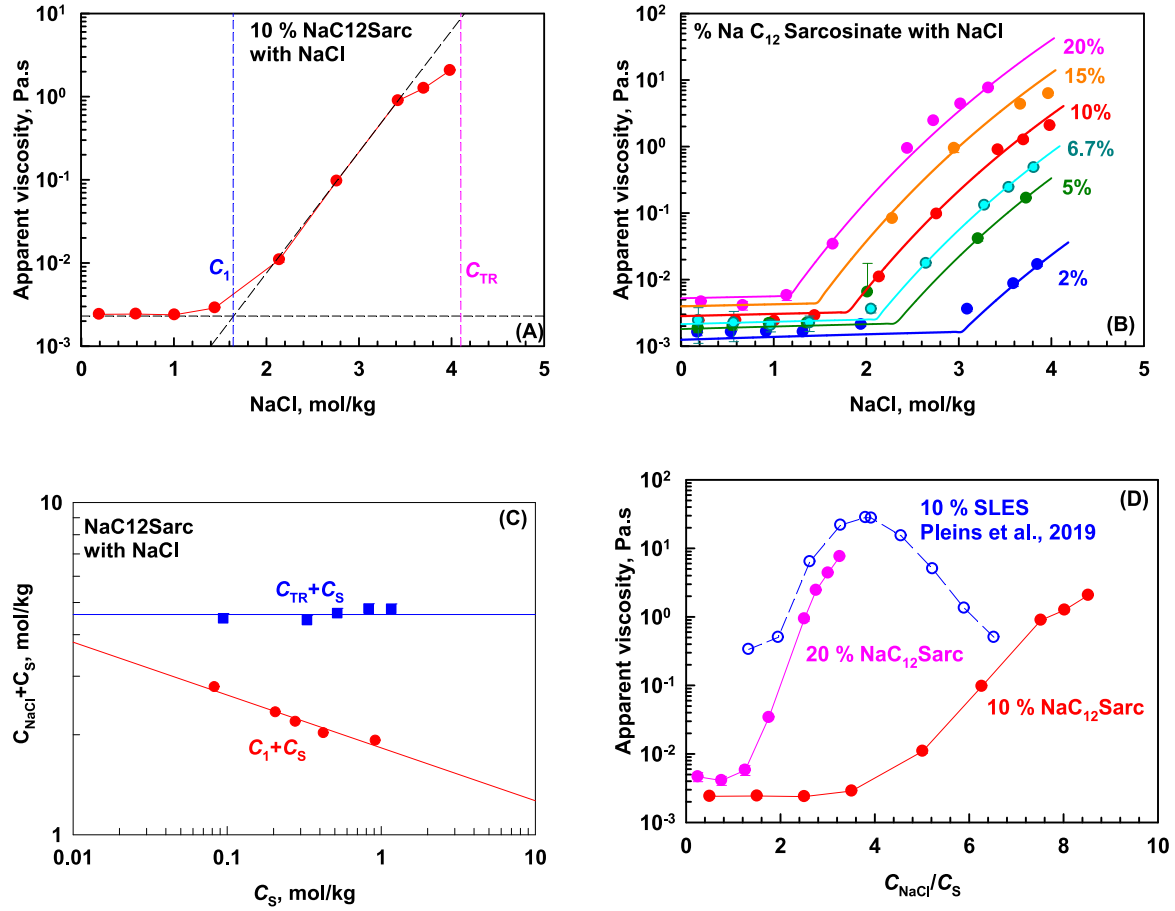

Fig. 1. (A) Apparent viscosity (Pa.s) as a function of NaCl concentration (mol/kg) for 10 wt% $NaC_{12}Sarcosinate$ solutions. The vertical blue dash line shows the threshold NaCl concentration, C_1, for inducing viscosity increase, the vertical pink dash line shows the threshold salt concentration for precipitation, C_{TR}; (B) Apparent viscosity as a function of NaCl concentration (mol/kg) at different $NaC_{12}Sarcosinate$ concentrations; Continuous curves are calculated according to Eqs. (6) and (7), whereas the points are experimental data for apparent viscosity measured at low shear rates for solutions with $C_{el} > C_1$. (C) Threshold NaCl concentrations for inducing viscosity increase, C_1 and threshold electrolyte concentration for precipitation, C_{TR} as a function of surfactant concentration, C_S; (D) Apparent viscosity vs the concentration ratio of added sodium chloride and surfactant concentration, C_{NaCl}/C_s for solutions prepared with 10 wt% $NaC_{12}Sarc$ and 20 wt% $NaC_{12}Sarc$ compared with the data for 10 % SLES taken from Pleins et al. [3]. (For interpretation of the references to colour in this figure legend, the reader is referred to the web version of this article.)

rates, the viscosity remains relatively constant up to a critical shear rate, after which it sharply decreases with a further increase in shear rate.

A comparison of the salt curves for 10 wt% and 20 wt% $NaC_{12}Sarc$ with the salt curve of 10 wt% sodium lauryl ether sulfate (SLES) from Pleins et al. [3] reveals that a higher sarcosinate concentration is needed to reach viscosity levels comparable to SLES solution at the same electrolyte-surfactant ratio, C_{NaCl}/C_S, see Fig. 1D. Moreover, the two surfactants exhibit different salt curve profiles. For SLES solutions, viscosity exhibits a maximum with increasing salt concentration, reflecting the micelle transformation from spherical at low C_{NaCl}, to wormlike micelles at a peak viscosity, to branched micelles beyond the maximum. In contrast, the salt curves of $NaC_{12}Sarc$ show only the initial steep increase in viscosity with increasing salt concentration, which corresponds to the formation of elongated micelles. When the critical concentration, C_{TR}, is reached, the crystal formation from the surfactant and the counterion becomes more favourable than the formation of branched micelles.

As a next step, we analyse the obtained results at different salt and surfactant concentrations by using the model developed by Pleines et al. [3] and Mitrinova et al. [11]. In this approach, the packing parameter is calculated assuming that the average area per molecule in the micelles can be calculated by the proportions of molecules in their neutral and ionized states [3]:

$$p = \frac{v}{(\alpha_1 a_{Sar^-} + (1-\alpha_1) a_{MSar})\, l} \tag{2}$$

where p is the packing parameter, v is the effective molecular volume of $NaC_{12}Sarc$, l is the surfactant length, α_1 is the fraction of $NaC_{12}Sarc$ molecules which are in ionized form, a_{Sar-} is the area per molecule for ionized sarcosinate molecules and a_{MSar} is the area per molecule of non-ionized $NaC_{12}Sarc$ molecule. The area per molecule for the neutralized molecule is calculated based on the surface tension isotherm determined by Petkova & Tcholakova [36] to be 0.42 nm^2. The area per molecule for the ionized form of the molecule is determined to be 0.8 nm^2 [36]. The volume of the tail is calculated by the Tanford Eq. [40] to be $v = 0.323$ nm^3 and $l = 1.545$ nm. For the calculation of α_1, the equilibrium between ionized and non-ionized molecules is assumed and the following expression proposed by Pleines et al. [3] is used:

$$C_{NaSar} = \frac{C_{NaCl} + C_S + K_1 - \sqrt{(C_{NaCl} + C_S + K_1)^2 - 4C_{NaCl}C_S}}{2} \tag{3}$$

$$\alpha_1 = \frac{C_{Sar^-}}{C_S} \tag{4}$$

$$K_1 = \frac{C_{Na^+} C_{Sar^-}}{C_{NaSar}} \tag{5}$$

where C_{NaSar} is the molality of neutralized $NaC_{12}Sarc$ molecules, C_{Sar-} is the molality of ionized sarcosinate molecules, C_{Na+} is the molality of free Na^+ which are not bound to sarcosinate molecules, C_{NaCl} is the molality of added NaCl in the solution and C_S is the molality concentration of $NaC_{12}Sarc$ dissolved in the solution.

At $C_{NaCl} < C_1$, the viscosity of $NaC_{12}Sarc$ solutions is calculated under the assumption that it increases linearly with C_S and C_{NaCl}:

$$\eta = (0.8901 + 0.11C_{NaCl} + 5C_S) \times 10^{-3} \qquad at\ C_{NaCl} < C_1 \tag{6}$$

The first part of the equation accounts for the viscosity of water at 25 °C, the second term accounts for the viscosity increase due to the increased NaCl concentration, in accordance with data reported in Ref. [41], the third term accounts for the viscosity increase due to the increased $NaC_{12}Sarc$ concentration. The viscosity in Eq. (6) is expressed in Pa.s and in the absence of dissolved NaCl and $NaC_{12}Sarc$, it gives the viscosity of water, which is 0.8901 mPa.s at 25 °C [41].

At $C_{NaCl} > C_1$, the viscosity of the solutions is scaled with C_S of power of 2.7 and depends on the packing parameter by the following expression:

$$\eta = C_S^{2.7} \exp(157.7p - 57.5) \qquad at\ C_{NaCl} \geq C_1 \tag{7}$$

where p is the packing parameter and C_S is the molality of $NaC_{12}Sarc$ concentration. Note that at $C_{NaCl} \geq C_1$ the higher value of viscosity calculated by Eq. (6) and Eq. (7) is used for the transition region. The scaled viscosity $\eta/C_S^{2.7}$ as a function of the packing parameter, which is calculated under the assumption that the dissociation constant of $NaC_{12}Sarc$, K_1, is 2 mol/kg, is shown in Fig. S4, whereas the predicted viscosities based on Eqs. (6) and (7) are shown as a function of NaCl concentration as continuous curves in Fig. 1B, together with the experimental data obtained at different $NaC_{12}Sarc$ concentrations. One sees that there is very good agreement between experimental data and theoretical predictions for all studied $NaC_{12}Sarc$ concentrations.

The used value for $K_1 = 2$ mol/kg for $NaC_{12}Sarc$ is more than 7-times higher than the respective value for SLES molecules (0.27 mol/kg [11]) showing that the interactions between Na^+ and sarcosinate ion are much weaker than the interactions between Na^+ and sulfate ion in SLES, which explains why much higher salt concentrations are required to induce the micelle growth for $NaC_{12}Sarc$ compared to SLES. On the other hand, the effect of surfactant concentration for elongated micelles (between C_1 and C_{TR}) is much stronger than that of SLES. In the current study the power law index is determined to be ≈2.7, whereas the value between 1.7 and 2 is reported for mixture of SLES+CAPB by Mitrinova et al. [11], which means that $NaC_{12}Sarc$ micelles are less multiconnected compared to SLES+CAPB micelles.

3.2. Effect of surfactant chain length (C12 vs C14 vs Cocoyl) and type of electrolyte used (NaCl vs KCl)

As a next step, we investigate the effect of surfactant chain length on the rheological behaviour by performing experiments with sodium myristoyl sarcosinate ($NaC_{14}Sarc$) and sodium cocoyl sarcosinate (NaCocoylSarc) at a fixed surfactant concentration of 10 wt%. The obtained salt curves in the presence of NaCl and KCl are shown in Fig. 2. It is seen that the onset of viscosity increase, C_1, is the lowest for $NaC_{14}Sarc$, intermediate for $NaC_{12}Sarc$ and the highest for NaCocoylSarc for both electrolytes. The values of C_1 are higher for KCl than for NaCl, indicating a lower ability of KCl to induce micelle elongation compared to NaCl. This finding is in good agreement with the data from the literature, which shows a greater tolerance of the carboxyl group towards K^+ compared to Na^+ [18,42,43] as well as to measured higher CMC for NaC12Sarc in presence of KCl than in presence of NaCl [31].

Interestingly, NaCocoylSarc solutions, in which the main components are $NaC_{12}Sarc$ (61.5 %) and NaC14Sarc (20.5 %), exhibit significantly higher tolerance to both Na^+ and K^+, with values of C_1 and C_{TR} being the highest among the surfactants studied. The most probable explanation for this unexpected result is the presence of low-chain sarcosinates (C8 and C10), which do not allow good packing of longer-chain sarcosinates and significantly increase the region in which the spherical micelles are formed in the solution. The dependence of C_1 on the chain length is shown in Fig. 2B. One sees that the values determined for NaCocoylSarc fall on the same curve as those obtained for $NaC_{12}Sarc$ and $NaC_{14}Sarc$ under the assumption that the chain length of NaCocoylSarc is 10C-atoms. Therefore, the mixed chain length strongly affects the phase behaviour of NaCocoylSarc. Similar behaviour is reported in [44] for cocoamidopropyl betaine (CAPB), a complex mixture of surfactants with different chain lengths, as NaCocoylSarc studied in the current work. It is shown that CAPB self-assembles into spherical micelles as CyAPB (C8) and CiAPB (C10), whereas LAPB (C12) and MAPB (C14) form ellipsoidal micelles [44].

The threshold salt concentrations, C_{TR}, for inducing phase separation are also shown in Fig. 2B. It is seen that the C_{TR} decreases with the increase in surfactant chain length. The values of C_{TR} determined for NaCocoylSarc in the presence of KCl and NaCl are equal to their

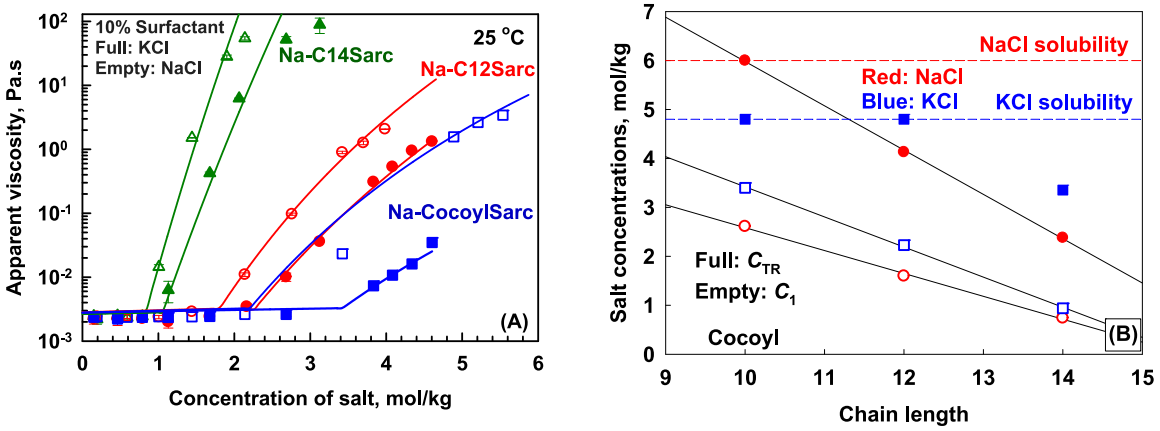

Fig. 2. (A) Apparent viscosity as a function of molarity of added salt: NaCl (empty points) and KCl (full points) for 10 wt% NaC_{14}Sarcosinate (green triangles), NaC_{12}Sarcosinate (red circles), NaCocoyl Sarcosinate (blue squares). The points are experimental data for apparent viscosity, the curves are theoretically calculated dependences according Eqs. (6) and (7). (B) Threshold salt concentrations for the onset of viscosity increase, C_1 (empty points) and for the formation of precipitates in the solutions, C_{TR} (full symbols) for NaCl (red circles) and KCl (blue squares) for 10 wt% surfactant solutions. The dashed lines represent the solubility limits of NaCl (red line) and KCl (blue line). The experimental points shown at chain length of 10 correspond to data obtained with sodium cocoyl sarcosinate. (For interpretation of the references to colour in this figure legend, the reader is referred to the web version of this article.)

solubility limits, as indicated by the dashed lines in Fig. 2B, and salt precipitates occur before the precipitation of the surfactants (Fig. S5). A similar behaviour is observed for NaC_{12}Sarc in the presence of KCl.

The solutions containing salt concentration between C_1 and C_{TR} are characterised by increased viscosity due to the formation of elongated micelles and after a certain point the formation of worm-like micelles. An indication for the formation of wormlike micelles in the solutions of NaC_{14}Sarc at high concentrations of the studied monovalent salts is that at high shear rates, all experimental curves merge around the same line with a slope close to −1 (Fig. S6B).

In order to describe the viscosity as a function of salt concentration, we use the approach described in Mitrinova et al. [11], which accounts for the competition between Na^+ coming from surfactant and K^+, which is added as KCl. The following expressions are used when KCl is added as a background electrolyte:

$$\alpha_1 = 1 - \frac{C_{NaSar} + C_{KSar}}{C_S} \tag{8}$$

where C_{KSar} is the molality of neutralized sarcosinate molecules by K^+, which is determined from the following set of equations:

$$K_1 = \frac{(C_S - C_{NaSar})(C_S - C_{NaSar} - C_{KSar})}{C_{NaSar}}$$
$$K_2 = \frac{(C_{KCl} - C_{KSar})(C_S - C_{NaSar} - C_{KSar})}{C_{KSar}} \tag{9}$$

where C_{KCl} is the molality of added KCl, K_2 is the dissociation constant of potassium sarcosinate (KSarcosinate). The experimental data are very well described under the assumption that the dissociation constant for KSarcosinate is 2.65 mol/kg, see continuous curves in Fig. 2A. The higher value of K_2 (KSarcosinate) than K_1 (NaSarcosinate) is related to the lower affinity of the carboxylic group for K^+ as compared to Na^+, which is in very good agreement with experimental data known from the literature [18,42]. The values of K_2 (KSarcosinate) = 2.65 mol/kg and K_1 (NaSarcosinate) = 2 mol/kg are used to calculate the adsorption energy of K^+ and Na^+ to the micellar surface of sarcosinate by using Eq. (16) from Ref. [11]. The binding energy of Na^+ to sarcosinate micelles is determined to be 1 k_BT, whereas for K^+, the adsorption is 0.8 k_BT. These values are significantly smaller than those determined for adsorption of these ions on the surface of SLES micelles, which were found to be 3.1 k_BT for Na^+ and 3.9 k_BT for K^+. The obtained results are in good agreement with those reported by Vlachy et al. [18], who demonstrated through molecular dynamics simulations that acetate preferentially binds sodium over potassium, whereas methylsulfate prefers potassium over sodium.

The area per molecule for neutralized NaSarc and KSarc is assumed to be the same and equal to 0.42 nm^2 for C_{12}Sarc and 0.25 nm^2 for C_{14}Sarc. These values are determined from the surface tension isotherms reported by Petkova and Tcholakova [36]. As can be seen, there is a very good description of the obtained experimental results with the theoretical predictions for C_{12}Sarcosinate and C_{14}Sarcosinate. The obtained results for the area per molecule in Ref. [36] for CocoylSarcosinate are very similar to those reported for C_{14}Sarcosinate. If these values are used, the description of the results from viscosity measurements is not good. The reason is that this compound contains long-chain surfactants that adsorb on the air-water interface and form a dense adsorption layer with an area per molecule of 0.25 nm^2. However, in the micelles, the presence of short-chain molecules significantly affects the packing. As a consequence, the area per molecule at which good agreement between experimental data and theoretical prediction is found is 0.45 nm^2 in the presence of Na^+ and 0.48 nm^2 in the presence of K^+. Note that a similar discrepancy between adsorption on the air-water interface and the type of micelles formed is reported for CAPB in Ref. [44]. Therefore, the area per molecule measured from surface tension isotherms can be used to predict micellar growth for individual surfactants. In contrast, when the homologues with different chain lengths are present in the solutions, the longer chain surfactants determine the area per molecule on the air-water interface, whereas the shorter chain surfactants are more important for the type of micelles formed and they determine the viscosity of the solutions in the presence of salt. From a practical viewpoint, this analysis shows that the longer chain homologues of alkyl sarcosinates can be used to build up the viscosity of the formulations at lower salt concentrations.

The maximum viscosity measured for the NaC_{14}Sarc solutions decreases from 88 Pa.s to 55 Pa.s as the hydrated counterion radius increases from Na^+ (0.331 nm) to K^+ (0.358 nm) (see Table S2). A similar decrease in the maximum viscosity in the salt curve upon increase of the radius of hydrated counterion is shown by Mitrinova et al. [10] for the SLES+CAPB system. Note that the opposite dependence is reported by Pleines et al. [3] for SLES system. This difference is related to the fact that in SLES+CAPB system the carboxylic group from CAPB interacts in a similar way with counterions as the carboxylic group from sarcosinate in the current study. On the other hand, when the sulfate group from SLES interacts with the counterions, the viscosity is higher when Na^+ is

used instead of K^+. Increasing the length of the hydrophobic tail results in a decrease in C_{TR}, allowing the viscosity to increase before reaching the solubility limit of the salt itself.

SAXS measurements were carried out to characterize the micelles formed in NaC_{12}Sarc and NaC_{14}Sarc solutions with two different NaCl concentrations – the lowest studied NaCl concentration at which the surfactant solutions have low viscosity and Newtonian behaviour, and the NaCl concentration at which the maximal viscosity of the solutions is reached before precipitation of the surfactant.

At low salt concentrations, both sarcosinates exhibit similar spectra, characterised by a broad peak representative of ellipsoidal micelles, as shown in Fig. 3. A leftward shift in the peak position is observed for myristoyl sarcosinate compared to lauryl, indicating bigger sizes. In addition, the slope of the curves at the low q-region for C_{12}Sarc approaches zero, which is typical for spherical objects, while for C_{14}Sarc it is around −0.7, representing elongated micelles [45].

The increase in salt concentration, up to the highest electrolyte concentration before precipitation, leads to a significant change in the spectra – the broad peak disappears and only the right-hand side shoulder remains. Such behaviour is observed for systems with screened electrostatic interactions between charged molecules in the micelles or between the micelles themselves in the presence of electrolyte or hydrotrope [46,47].

Further, the SAXS spectra were evaluated through modelling via SASView software to determine the micellar parameters. The best fit was obtained by applying a core-shell model with accounting for electrostatic interactions. The scattering length density (SLD) of the hydrophobic chains and hydrophilic head groups was determined by using the following calculator: https://www.ncnr.nist.gov/resources/activation/. The SLD of the C_{12}Sarc core was set as for dodecane (7.34×10^{-6} A^{-2}), while for C_{14}Sarc as tetradecane (7.45×10^{-6} A^{-2}). The SLD of solvent was chosen as for water: 9.47×10^{-6} A^{-2}. As shown in Fig. 3 and Table 1, the model fit is better for samples with higher salt concentrations. Myristoyl sarcosinate possesses bigger micelles compared to shorter-chained analogue. The same is true for higher electrolyte concentration, which explains the higher measured viscosity upon salt addition for both studied surfactants.

3.3. Effect of different types of co-surfactants on the properties of NaC_{12}Sarcosinate solution

The solutions of NaC_{12}Sarc + co-surfactant without added salt are isotropic, with low viscosity and Newtonian rheological behaviour (Table S1). The effect of different types of co-surfactants on the salt curves of NaC_{12}Sarc with NaCl is shown in Fig. 4. It is seen that the amphoteric surfactant CAPB does not significantly affect the viscosity of NaC_{12}Sarc solutions at different NaCl concentrations. There is a slight increase in the C_{TR} and the maximal viscosity reached before precipitation of the surfactants (Table S3). When the C_{TR} is reached, precipitation of the surfactants with the sodium counterions is observed (Fig. S7). The lack of any effect of replacing sarcosinate with CAPB is related to the fact that both molecules have a carboxyl group at the end of their hydrophilic head, which interacts with sodium counterions in a similar way, despite the differences in the internal part of the hydrophilic head. On the other hand, the amphoteric surfactants *N*-dodecyl-*N*,*N*-dimethyl-3-ammonio-1-propanesulfonate (Sulfo Betaine) and decylamine oxide (Ammonyx) shift the salt curve to the right, i.e., higher concentrations of NaCl are required to increase the viscosity of mixed surfactant solutions compared to sarcosinate solutions without co-surfactants. Sulfo Betaine does not alter the maximum reached viscosity before phase separation, whereas Ammonyx lowers the maximum viscosity. Note that in the presence of both co-surfactants, the solubility limit of NaCl is reached, and the salt precipitates before precipitation of the surfactant (Fig. S7B, C). This shift of the curve to the right is most probably related to the reduced concentration of NaC_{12}Sarc in the solution and the lack of strong interaction with the studied co-surfactants.

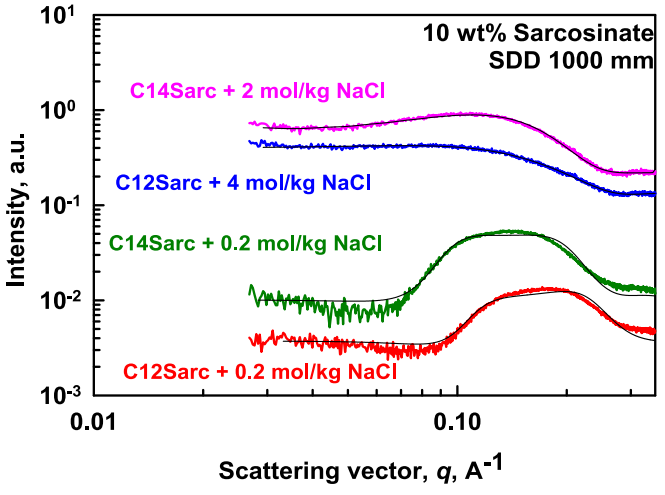

Fig. 3. Intensity as a function of scattering vector from SAXS measurements of 10 wt% NaC_{12}Sarcosinate and NaC_{14}Sarcosinate with NaCl. The concentrations of the electrolytes are denoted in the graph. The sample-to-detector distance is 1000 mm. Black lines represent the fit of the data with the core-shell ellipsoid model.

Table 1
The characteristics of the micelles, as determined by SAXS analysis using the core-shell ellipsoid model.

Sarcosinate	NaCl, mol/kg	Slope	Rx, nm	Ry, nm	Ry/Rx	Fitting error, χ
C_{12}Sarc	0.2	0.2	2.5	3.0	1.23	0.0170
	4		2.3	4.1	1.74	0.0007
C_{14}Sarc	0.2	−0.7	2.7	3.6	1.32	0.0217
	2		3.0	32.5	10.9	0.0015

The nonionic co-surfactants cocamide monoethanolamine (CMEA), 1-octanol (C8Alc) and 1-octanoic acid (C8Ac) shift the salt curve of NaC_{12}Sarc and NaC_{12}Sarc + CAPB 2:1 to the left due to their smaller area of the hydrophilic head group. Lower salt concentrations are required for the micelles to change and to increase the viscosity of these solutions compared to NaC_{12}Sarc solutions. However, precipitation of the surfactants occurs in the solution of NaC_{12}Sarc + CMEA before reaching a peak in viscosity. On the other hand, the viscosity passes through a maximum with increasing NaCl concentration in the presence of C8Alc, C8Ac and CAPB+C8Alc. The peaks in the viscosity of the solutions with the alcohol and the acid are still lower than the maximal viscosity of the NaC_{12}Sarc solution reached before C_{TR}. This result could be related to the higher flexibility of the mixed micelle. After the viscosity maximum, branched micelles are formed and they are no longer able to solubilise the alcohol and the acid. As a result, we observe the separation of a second phase (Fig. S7E, F, G). The further increase of the NaCl concentration does not change the visual appearance of the solutions and the volume of the lower phase increases slightly (Fig. S8). When the NaCl concentration reaches 5 mol/kg, the solution of NaC_{12}Sarc + C8Alc becomes white and we observe the formation of multilamellar vesicles and other structures that appear with colours under polarised light.

Similar to CAPB, the cationic co-surfactants decyl, dodecyl and cetyltrimethylammonium bromide (C10TAB, DTAB and CTAB, respectively) do not affect the rheological properties of NaC_{12}Sarc and the salt curves in the presence of these surfactants are similar to the salt curve in the absence of co-surfactant. It should be noted, however, that in the mixtures with cationic surfactants, the sarcosinate concentration decreases from 10 wt% to 9.1 wt% due to the replacement of about 9 % of sarcosinate by cationic surfactant. In contrast, in the case of CAPB, the sarcosinate concentration decreases to 6.67 wt%. In other words,

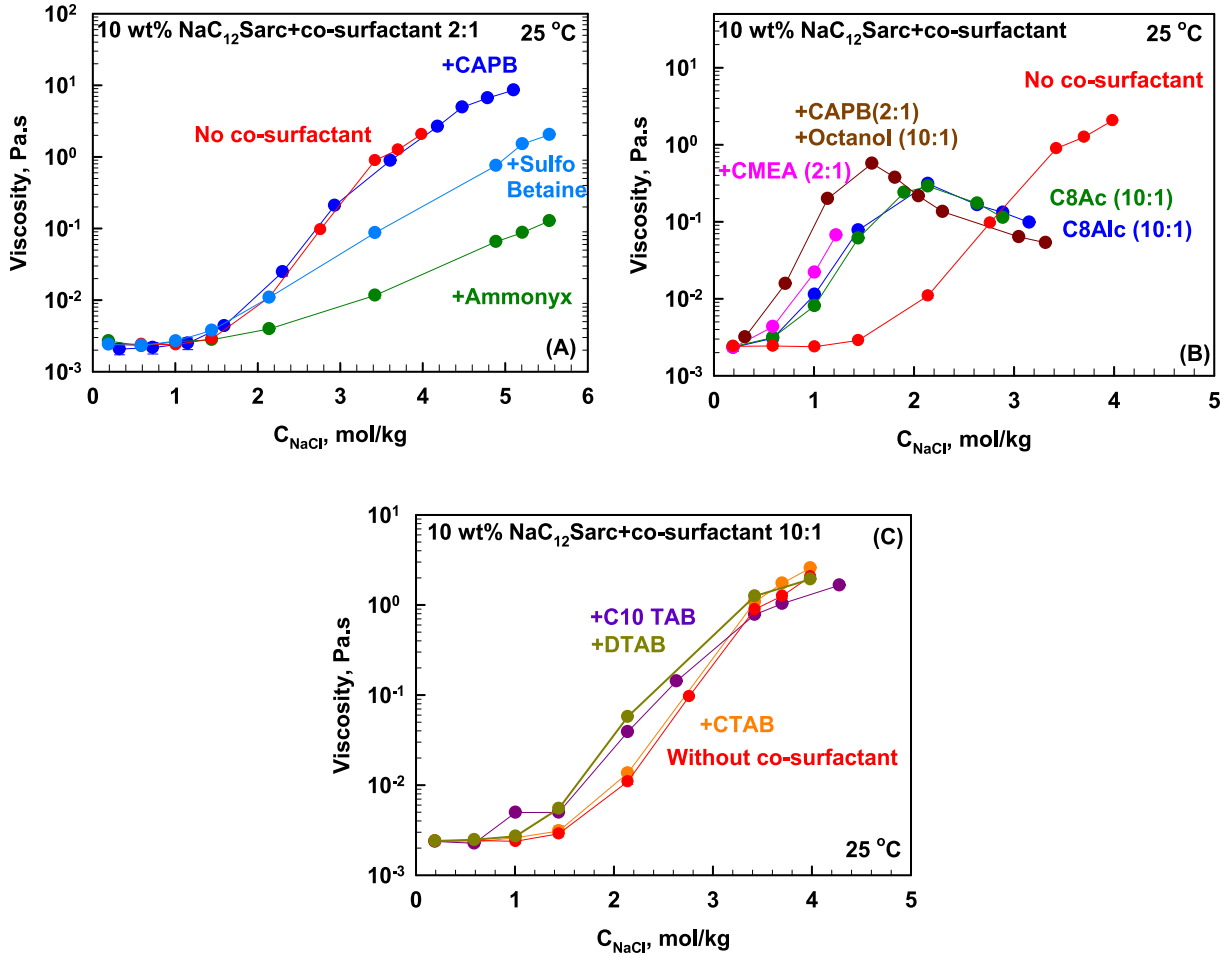

Fig. 4. Apparent viscosity as a function of molarity of added NaCl for 10 wt% NaC_{12}Sarcosinate and different co-surfactants. (A) Amphoteric co-surfactants; (B) Nonionic co-surfactants; (C) Cationic co-surfactants. The ratio of NaC_{12}Sarcosinate to co-surfactant is indicated in the graphs.

cationic surfactants do not have a significant effect on the salt curves because their concentration is too low to induce a change in the shape of the micelles. On the other hand, the lack of a strong effect of CAPB is associated with the formation of mixed micelles with sarcosinate, which, however, have very similar properties to the micelles of pure sarcosinate. Vu et al. [30] show that increasing the concentration of the cationic surfactant cetyl trimethyl ammonium chloride from 1 % to 3 % leads to a significant increase in the viscosity of the solution with 6 % NaC_{12}Sarc + 9 % cocoamidopropyl hydroxysultaine at natural pH (7.5).

^{1}H NMR, ^{13}C NMR and DOSY NMR measurements were carried out to confirm that sarcosinate and CAPB molecules form mixed micelles. We also investigated the mixed surfactant solution of sarcosinate and Ammonyx to understand what causes the lower maximal viscosity and higher C_{TR} compared to the 10 wt% sarcosinate solution. There are two possible reasons: (1) the two surfactants do not form mixed micelles and the observed effects are related to the lower concentration of the sarcosinate (6.67 wt%) in the mixture or (2) the two surfactants form mixed micelles but their heads are not able to come closer with the increase of NaCl concentration due to steric hindrance from the side -CH_3 groups in both surfactant molecules.

The ^{1}H NMR spectra of the solutions with CAPB and Ammonyx in the presence of 1.4 mol/kg NaCl are presented in Figs. S9 and S10, respectively. There is only a slight change in the chemical shift of the signal corresponding to the NH proton in the CAPB molecule. In the CAPB spectrum, the NH signal appears at 8.14 ppm, whereas in the mixture of CAPB and sarcosinate, it shifts to 8.22 ppm (see Table S4 in the Supporting Information). Although the changes in the chemical shifts of other CAPB signals are minimal, this variation, along with the small differences observed in the chemical shifts of certain sarcosinate signals before and after mixing with CAPB (3.88 ppm vs. 3.87 ppm; 2.40 ppm vs. 2.39 ppm; 2.27 ppm vs. 2.26 ppm; see Table S4), indicates the formation of mixed micelles. This conclusion is further supported by the chemical shifts observed in the ^{13}C NMR spectra (see Fig. 5, Fig. S11 and Table S5). The carboxylate carbonyl, which appears at 176.39 ppm in the sarcosinate solution, shifts by 35.2 Hz in the mixed solution with CAPB. The amide carbonyls, which appear at 175.18 in the sarcosinate solution shifts by 23 Hz. A significant chemical shift of 60.7 Hz is detected for the carbonyl (C═O) carbon in the carboxylate functional group of CAPB when mixed with sarcosinate. The carbon atoms in the surfactant tail of sarcosinate are only slightly affected by the presence of CAPB in the mixture, with their chemical shifts ranging between 6 and 7 Hz. Likewise, the carbon atoms in the CAPB tail are only slightly influenced by the presence of the sarcosinate molecule, as expected, since the tails of the two surfactants are structurally similar. From these data, we conclude that sarcosinate and CAPB form mixed micelles, further supported by the DOSY data presented below.

In the mixed surfactant solution of sarcosinate and Ammonyx, ^{1}H NMR shows that hydrogen atoms in the sarcosinate molecule, as well as those in Ammonyx, are only slightly affected after mixing, with chemical shifts ranging between 0.01 and 0.02 ppm (see Table S4). However, significant chemical shifts between 30 and 50 Hz are observed in the ^{13}C NMR spectra for the carboxylate carbonyl and amide carbonyl of sarcosinate after mixing with Ammonyx (see Fig. 6, Fig. S12 and Table S5), indicating the formation of mixed micelles. Additionally, small differences are observed in the chemical shifts of carbon signals from the terminal methyl groups in the aliphatic tails of sarcosinate and

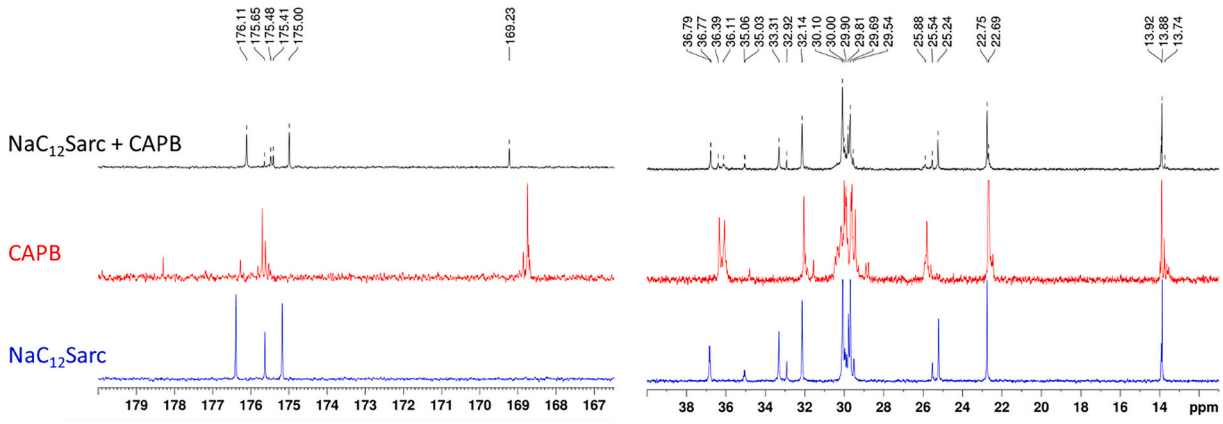

Fig. 5. Selected regions of ^{13}C NMR spectra of the solution of 10 wt% $NaC_{12}Sarc$ + CAPB 2:1 (black), 10 wt% $NaC_{12}Sarc$ (blue) and 10 wt% CAPB (red) in the presence of 1.4 mol/kg NaCl. (For interpretation of the references to colour in this figure legend, the reader is referred to the web version of this article.)

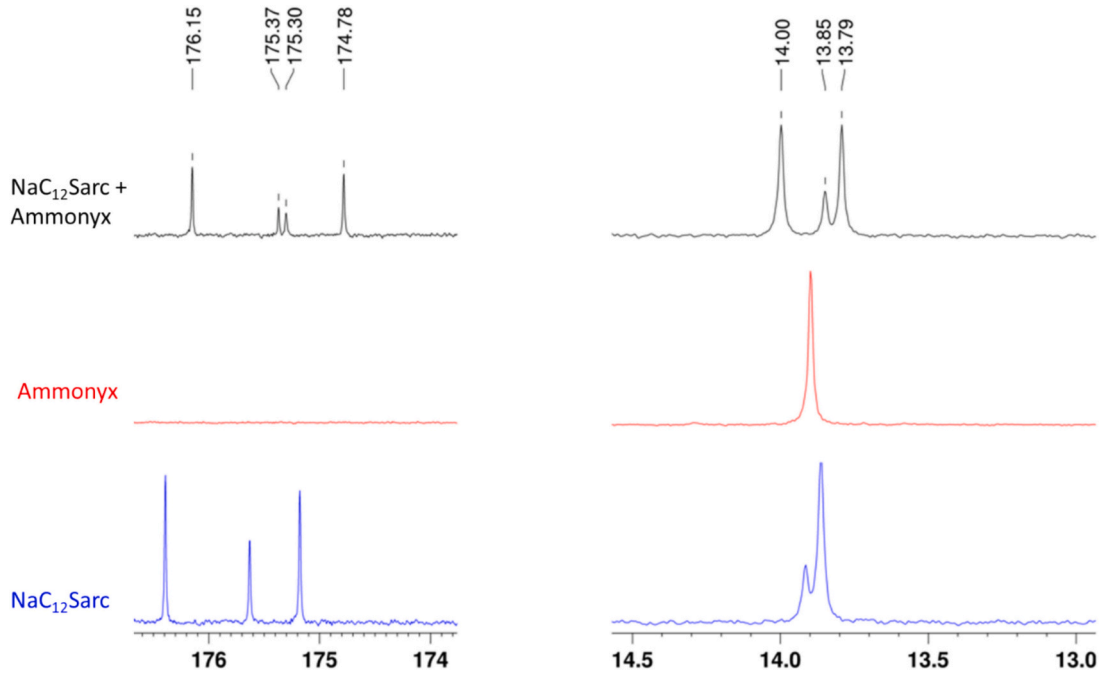

Fig. 6. Selected regions of ^{13}C NMR spectra of the solution of 10 wt% $NaC_{12}Sarc$ + Ammonyx 2:1 (black), 10 wt% $NaC_{12}Sarc$ (blue) and 10 wt% Ammonyx (red) in the presence of 1.4 mol/kg NaCl. (For interpretation of the references to colour in this figure legend, the reader is referred to the web version of this article.)

Ammonyx in their mixture, as shown in Fig. 6. Therefore, based on these observations, we conclude that sarcosinate and Ammonyx form mixed micelles.

In order to unambiguously confirm that sarcosinate forms mixed micelles with CAPB and Ammonyx, we acquired DOSY NMR spectra of the solutions of the different surfactants and their mixtures with different concentrations (Figs. S13 and S14). The DOSY NMR spectra of the corresponding mixtures at 10 % concentration are given in Fig. 7. One can see that the particular signals from Sarcosinate, CAPB, or Ammonyx have the same diffusion coefficient, which is evidence of the formation of mixed micelles. This statement is supported by the results obtained from the additional DOSY experiments conducted at different surfactant concentrations. As seen in Figs. S13 and S14, even at different concentrations and thus different diffusion coefficients of the mixtures, the signals from separate surfactants have the same diffusion coefficients. In the case of Sarcosinate and CAPB the newly formed micelles have a smaller diffusion coefficient than the micelles of the individual surfactants (Fig. S15A), while in the case of Sarcosinate and Ammonyx, the diffusion coefficient of the mixed micelles corresponds to the diffusion coefficient of sarcosinate and have smaller value than *D* of the Ammonyx (Fig. S15B). The exact values are presented in Table 2.

3.4. *Effect of electrolyte type on the properties of sarcosinate + CAPB solutions*

The results from the previous section showed that from all studied co-surfactants, an additional increase in the maximal viscosity of $NaC_{12}Sarc$ solution is observed only in the presence of CAPB. The same is true for the other two studied sarcosinates, as seen in Fig. 8. The maximal viscosity of $NaC_{14}Sarc$ + CAPB solution is 68.5 Pa.s (Table S6), whereas in the absence of the co-surfactant, it is 54.5 Pa.s. Even an outline of a maximum is observed in the salt curve of $NaC_{14}Sarc$ + CAPB. However, the subsequent increase in salt concentration leads to precipitation in the solution instead of the typical decrease in viscosity due to a transition in the micelle shape, as observed in the works of Mitrinova et al. [10] for the SLES+CAPB system and of Warmbier-

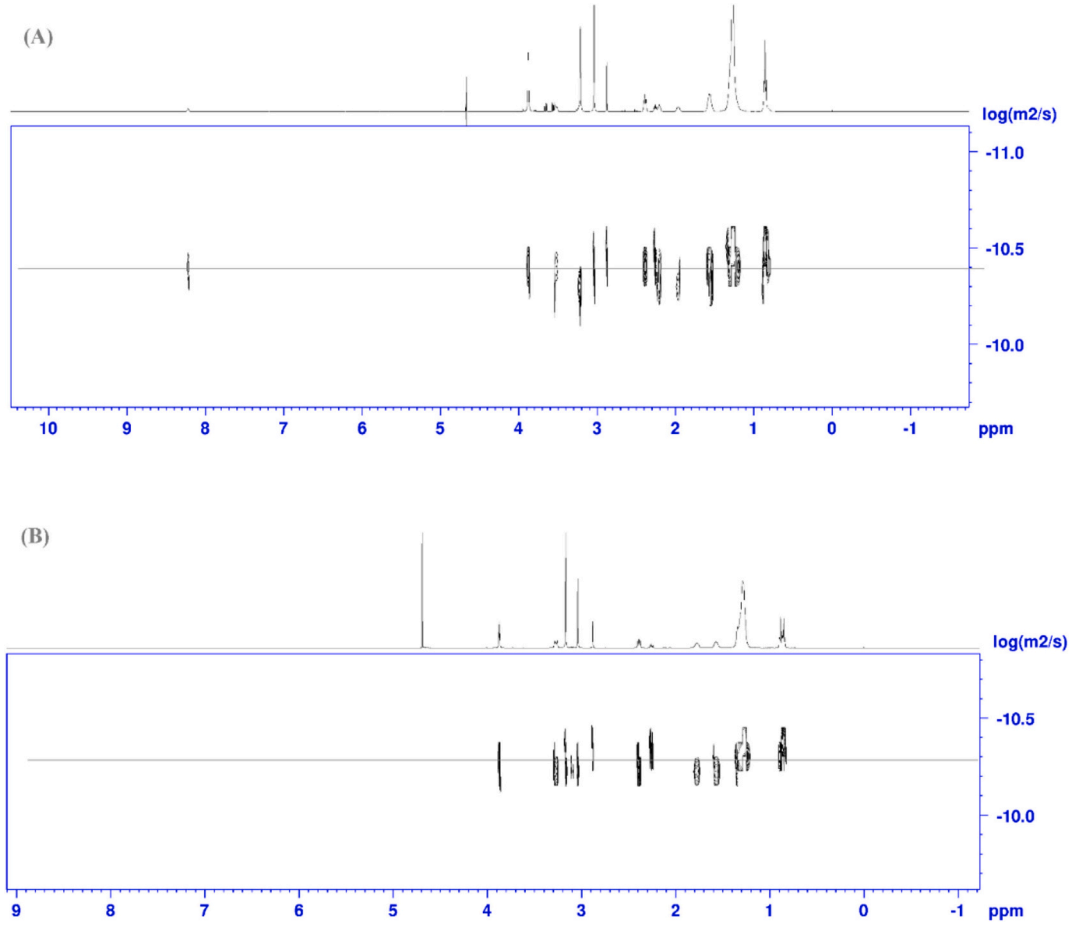

Fig. 7. DOSY NMR spectra of solutions of (A) 10 wt% $NaC_{12}Sarc$ + CAPB 2:1 and (B) 10 wt% $NaC_{12}Sarc$ + Ammonyx 2:1.

Table 2
Diffusion coefficients of $NaC_{12}Sarc$, CAPB, Ammonyx and their mixed micelles in the solutions with 10 wt% surfactant and 1.4 mol/kg NaCl.

10 % Surfactant + 1.4 mol/kg NaCl	η, mPa.s	D, $\mu m^2/s$	R_H (Stokes–Einstein–Sutherland equation), nm	
			For $\eta = 0.9$ mPa.s	For η of solution
$NaC_{12}Sarc$	2.9	48	5.1	1.6
CAPB	2.4	46	5.3	2.0
Ammonyx	2.6	54	4.5	1.6
$NaC_{12}Sarc$ + CAPB	4.4	41	5.9	1.2
$NaC_{12}Sarc$ + Ammonyx	2.8	46	5.3	1.7

Wytykowska et al. [23] for the CAPB+dodecylbenzenesulfonate system. The NaCl concentration required for phase separation increases in the presence of CAPB compared to solutions of myristoyl and cocoyl sarcosinate without the co-surfactant. The effect of CAPB on the viscosity of the mixture with NaCocoylSarc is the weakest because the solubility limit of NaCl is reached and the increase of the viscosity is interrupted (Table S6, Fig. S16A).

The influence of KCl on the rheological properties of $NaC_{12}Sarc$ solutions in the presence and absence of CAPB is compared in Fig. 9. The general conclusions about the effect of the type of electrolyte on the properties of the sarcosinate solutions are also valid for the mixtures of sarcosinate+CAPB. Similar salt curves are obtained for $NaC_{12}Sarc$ and $NaC_{12}Sarc$ + CAPB (2:1) with KCl. The maximal viscosity of the solutions is again higher in the presence of CAPB, whereas C_{TR} does not change since $C_{TR} \geq$ concentration of the saturated salt solution.

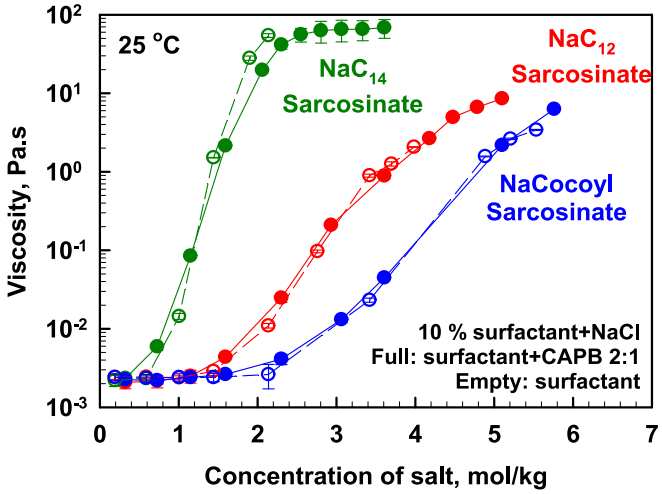

Fig. 8. Apparent viscosity as a function of molarity of added NaCl for 10 wt% NaC_{12}Sarcosinate + CAPB 2:1, Na-C_{14}-Sarcosinate+CAPB 2:1, Na-Cocoyl Sarcosinate+CAPB 2:1. Full symbols represent results in the presence of CAPB, and empty symbols – without CAPB.

4. Conclusions

Systematic experiments were performed to determine the viscosity response of three alkyl sarcosinate solutions (dodecyl, tetradecyl, and cocoyl) in the presence of two background electrolytes (NaCl and KCl) at pH > 6 where the alkyl sarcosinate molecules are in their ionized form.

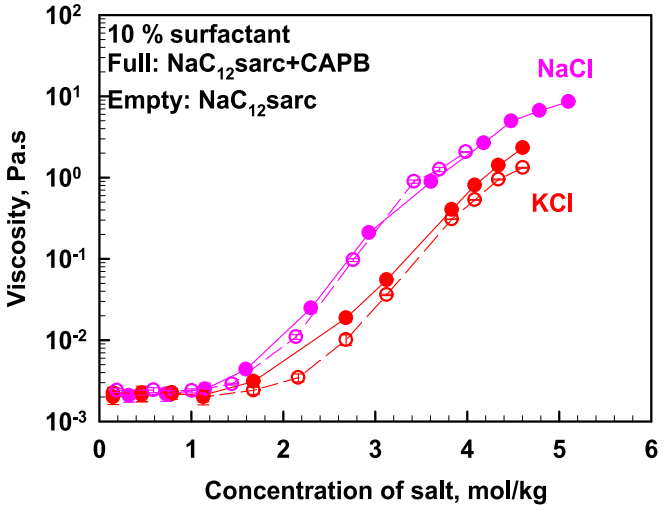

Fig. 9. Apparent viscosity as a function of molarity of added NaCl and KCl for 10 wt% NaC_{12}Sarcosinate + CAPB 2:1. Full symbols represent results in the presence of CAPB, and empty symbols – without CAPB.

The results revealed two well-defined regions in the salt curves. At low electrolyte concentrations, the solutions exhibit Newtonian behaviour with low viscosity. At intermediate concentrations of monovalent counterions, elongated micelles form, increasing viscosity while maintaining isotropic properties. At high concentrations, crystal formation occurs.

The limiting salt concentration for micelle growth, C_1, increases as the surfactant chain length shortens from C14 to C12. The presence of C8 and C10 sarocinate molecules in cocoyl sarcosinate further increases the value of C_1. The value of C_1 is lower for Na^+ than for K^+ due to the lower adsorption energy of K^+ (0.8 vs. 1 k_BT) on the micelle surface. In dodecyl and cocoyl sarcosinate solutions, KCl reaches its solubility limit before KSarcosinate precipitation occurs. The highest viscosity (88 Pa.s) is observed in sodium tetradecyl sarcosinate solutions with potassium chloride. A theoretical expression was derived and tested against experimental data, demonstrating excellent agreement between measured and predicted viscosities across different surfactant and salt concentrations.

Replacing 33 % of the alkyl sarcosinates with zwitterionic surfactants (CAPB, SulfoBetaine, or decylamine oxide) preserves the overall salt curve behaviour but alters the precipitation limit and maximum viscosity. CAPB increases the maximal viscosity due to the formation of mixed micelles with sarcosinate, which retain carboxyl groups on their surface. Conversely, decylamine oxide reduces maximal viscosity because steric hindrance from the side methyl groups prevents sufficient micelle elongation.

Substituting 33 % of lauroyl sarcosinate with the nonionic surfactant cocamide monoethanolamine (CMEA) significantly lowers the precipitation threshold and reduces maximum viscosity. A similar effect is observed when 9 % of lauroyl sarcosinate is replaced with octanoic acid or octanol, resulting in droplet formation rather than crystal formation after phase separation. However, replacing 9 % of lauroyl sarcosinate with cationic surfactants (C10TAB, DTAB, or CTAB) does not affect the salt curve or the maximum viscosity reached before precipitation.

The practical significance of the current study lies in the finding that longer-chain alkyl sarcosinates (such as tetradecyl, as investigated here) can achieve significantly higher viscosities at lower salt concentrations compared to shorter-chain analogs or mixtures of surfactants. The scientific significance stems from the development of a theoretical model capable of predicting the viscosity of alkyl sarcosinate solutions across a range of surfactant and salt concentrations. This study also explains the inability of cocoamidopropyl betaine to promote micellar growth in alkyl sarcosinate systems.

The limitations of this study are related to the behaviour of sarcosinate solutions in the presence of monovalent counterions at room temperature. The presence of divalent ions, such as Mg^{2+} and Ca^{2+}, is expected to significantly impact the phase behaviour of alkyl sarcosinates. Stronger interactions between these ions and the carboxylic group may result in precipitation before the formation of worm-like micelles. Another important factor not considered in this study is temperature, which could also significantly influence the rheological response of sarcosinate solutions.

CRediT authorship contribution statement

Dilek Gazolu-Rusanova: Writing – original draft, Visualization, Methodology, Formal analysis. **Marina Stoeva:** Visualization, Validation, Investigation, Formal analysis. **Zlatina Mitrinova:** Visualization, Investigation, Formal analysis. **Nevena Pagureva:** Visualization, Investigation, Formal analysis. **Nikola Burdzhiev:** Visualization, Investigation, Formal analysis. **Slavka Tcholakova:** Writing – review & editing, Visualization, Supervision, Funding acquisition, Formal analysis, Conceptualization.

Funding

This study was funded by the European Union-NextGenerationEU, through the National Recovery and Resilience Plan of the Republic of Bulgaria, project No. BG-RRP-2.004-0008.

Declaration of competing interest

The authors declare that they have no known competing financial interests or personal relationships that could have appeared to influence the work reported in this paper.

Acknowledgments

The support of the Centre of Competence “Sustainable Utilization of Bio-resources and Waste of Medicinal and Aromatic Plants for Innovative Bioactive Products” (BIORESOURCES BG), project BG16RFPR002-1.014-0001, funded by the Program “Research, Innovation and Digitization for Smart Transformation” 2021-2027, co-funded by the EU, is greatly acknowledged.

Appendix A. Supplementary data

Supplementary data to this article can be found online at https://doi.org/10.1016/j.molliq.2025.128069.

Data availability

Data will be made available on request.

References

[1] A. Parker, W. Fieber, Viscoelasticity of anionic wormlike micelles: effects of ionic strength and small hydrophobic molecules, Soft Matter 9 (2013) 1203–1213.
[2] J.H. Mu, G.Z. Li, X.L. Jia, H.X. Wang, G.Y. Zhang, Rheological properties and microstructures of anionic micellar solutions in the presence of different inorganic salts, J. Phys. Chem. B 106 (2002) 11685–11693.
[3] M. Pleines, W. Kunz, T. Zemb, D. Benczedi, W. Fieber, Molecular factors governing the viscosity peak of giant micelles in the presence of salt and fragrances, J. Colloid Interface Sci. 537 (2019) 682–693.
[4] R. Oda, J. Narayanan, P.A. Hassan, C. Manohar, R.A. Salkar, F. Kern, S.J. Candau, Effect of the Lipophilicity of the counterion on the viscoelasticity of micellar solutions of cationic surfactants, Langmuir 14 (1998) 4364–4372.
[5] W.J. Kim, S.M. Yang, M. Kim, Additive effects on the microstructure evolution in hexadecyltrimethylammonium bromide solution and its rheological properties, J. Colloid Interface Sci. 194 (1997) 108–119.
[6] S.R. Raghavan, G. Fritz, E.W. Kaler, Wormlike micelles formed by synergistic selfassembly in Mixtures of anionic and cationic surfactants, Langmuir 18 (2002) 3797–3803.

[7] T.R. Desai, S.G. Dixit, Interaction and viscous properties of aqueous solutions of mixed cationic and nonionic surfactants, J. Colloid Interface Sci. 177 (1996) 471–477.
[8] N.C. Christov, N.D. Denkov, P.A. Kralchevsky, K.P. Ananthapadmanabhan, A. Lips, Synergistic sphere-to-rod micelle transition in mixed solutions of sodium dodecyl sulfate and cocoamidopropyl betaine, Langmuir 20 (2004) 565–571.
[9] S. Anachkov, G. Georgieva, L. Abezgauz, D. Danino, P. Kralchevsky, Viscosity peak due to shape transition from wormlike to disklike micelles: effect of dodecanoic acid, Langmuir 34 (2018) 4897–4907, https://doi.org/10.1021/acs.langmuir.8b00421.
[10] Z. Mitrinova, H. Alexandrov, N. Denkov, S. Tcholakova, Effect of counter-ion on rheological properties of mixed surfactant solutions, Colloids Surf. A 643 (2022) 128746.
[11] Z. Mitrinova, Z. Valkova, S. Tcholakova, Interplay between cosurfactants and electrolytes for worm-like micelles formation, Colloids Surf. A 707 (2025) 135943, https://doi.org/10.1016/j.colsurfa.2024.135943.
[12] R. Zana, E. Kaler, Giant Micelles: Properties and Applications, CRC Press, Boca Raton, FL, 2007.
[13] T. Vu, P. Koenig, B.M. Cochran, K.P. Ananthapadmanabhan, M. Weaver, B. Reeder, H.D. Hutton, G.B. Kasting, Thickening mechanisms for an amino acid-derived surfactant composition, Colloids Surf. A Physicochem. Eng. Asp. 589 (2020) 124424.
[14] A. Khatory, F. Lequeux, F. Kern, S.J. Candau, Linear and nonlinear viscoelasticity of semidilute solutions of wormlike micelles at high salt content, Langmuir 9 (1993) 1456–1464.
[15] A. Khatory, F. Kern, F. Lequeux, J. Appell, G. Porte, N. Morie, A. Ott, W. Urbach, Entangled versus multiconnected network of wormlike micelles, Langmuir 9 (1993) 933–939.
[16] P.J. Missel, N.A. Mazer, M.C. Carey, G.B. Benedek, Influence of alkali-metal counterion identity on the sphere-to-rod transition in alkyl sulfate micelles, J. Phys. Chem. 93 (1989) 8354–8366.
[17] L. Ziserman, L. Abezgauz, O. Ramon, S.R. Raghavan, D. Danino, Origins of the viscosity peak in wormlike micellar solutions. 1. Mixed catanionic surfactants. A cryo-transmission electron microscopy study, Langmuir 25 (18) (2009) 10483–10489, https://doi.org/10.1021/la901189k.
[18] N. Vlachy, B. Jagoda-Cwiklik, R. V'acha, D. Touraud, P. Jungwirth, W. Kunz, Hofmeister series and specific interactions of charged headgroups with aqueous ions, Adv. Colloid Interf. Sci. 146 (2009) 42–47.
[19] W. Kunz, J. Henle, B.W. Ninham, 'Zur Lehre von der Wirkung der Salze' (about the science of the effect of salts): Franz Hofmeister's historical papers, Curr. Opin. Colloid Interface Sci. 9 (2004) 19–37.
[20] K. Singh, D.G. Marangoni, J.G. Quinn, R.D. Singer, Spontaneous vesicle formation with an ionic liquid amphiphile, J. Colloid Interface Sci. 335 (2009) 105–111.
[21] S. Lifshiz-Simon, W. Kunz, T. Zemb, Y. Talmon, Ion effects on co-existing pseudo-phases in aqueous surfactant solutions: cryo-TEM, rheometry, and quantification, J. Colloid Interface Sci. 660 (2024) 177–191.
[22] L. Zhou, Z. Liu, Y. Wang, Molecular insights: how counterions determine surfactant aggregation, Adv. Colloid Interf. Sci. 341 (2025) 103484.
[23] E. Warmbier-Wytykowska, A.P. Williams, J. Rozanski, P. Fischer, V. Lutz-Bueno, S. Handschin, L. Baraldi, J. Warmbier, P. Wagner, S. Różańska, How do the valency and radii of cations affect the rheological properties of aqueous solutions of zwitterionic and anionic surfactant mixtures? Langmuir 41 (2025) 3561–3571.
[24] K.D. Collins, G.W. Neilson, J.E. Enderby, Ions in water: characterizing the forces that control chemical processes and biological structure, Biophys. Chem. 128 (2007) 95–104.
[25] P. Clapés, M. Rosa Infante, Amino acid-based surfactants: enzymatic synthesis, properties and potential applications, Biocatal. Biotrans. 20 (2002) 215–233.
[26] R. Bordes, K. Holmberg, Amino acid-based surfactants – do they deserve more attention? Adv. Colloid Interf. Sci. 222 (2015) 79–91.
[27] I.A. Nnanna, J. Xia, Protein-based surfactants: synthesis, physicochemical properties, and applications, in: A.T. Hubbard (Ed.), Surfactant Science Series, Marcel Dekker, New York, 2001.
[28] L. Rhein, Surfactant action on skin and hair: cleansing and skin reactivity mechanisms, in: I. Johansson, P. Somasundaran (Eds.), Handbook for Cleaning/Decontamination of Surfaces, Elsevier Science B.V., Amsterdam, The Netherlands, 2007, https://doi.org/10.1016/B978-044451664-0/50009-7.
[29] K.P. Ananthapadmanabhan, Amino-acid surfactants in personal cleansing (review), Tenside Surfactant Deterg. 56 (5) (2019) 378–386.
[30] T. Vu, P. Koenig, M. Weaver, H.D. Hutton, G.B. Kasting, Effects of cationic counterions and surfactant on viscosity of an amino acid-based surfactant system, Colloids Surf. A Physicochem. Eng. Asp. 626 (2021) 127040, https://doi.org/10.1016/j.colsurfa.2021.127040.
[31] G.B. Ray, S. Ghosh, S.P. Moulik, Physicochemical studies on the interfacial and bulk behaviors of sodium N-dodecanoyl sarcosinate (SDDS), J. Surfactant Deterg. 12 (2) (2009) 131–143, https://doi.org/10.1007/s11743-008-1105-3.
[32] D. Varade, P. Bahadur, Interaction in mixed micellization of sodium N-tetradecanoylsarcosinate with ionic and nonionic surfactants, J. Dispers. Sci. Technol. 26 (5) (2005) 549–554.
[33] H. Lu, M. Yuan, B. Fang, J. Wang, Y. Guo, Wormlike micelles in mixed amino acid-based anionic surfactant and zwitterionic surfactant systems, J. Surfactant Deterg. 18 (4) (2015) 589–596, https://doi.org/10.1007/s11743-015-1683-9.
[34] D. Varade, G. Rajput, D.S. Janni, G. Subramanyam, Rheology and surface active properties of sodium N-lauroyl sarcosinate in mixed surfactant system, Colloids Surf. A 697 (2024) 134349, https://doi.org/10.1016/j.colsurfa.2024.134349.
[35] X. Liu, K. Wu, W. Song, Q. Lei, H. Zhang, J. Pan, X. Ge, Aqueous solution thickening of amino acid-based surfactant by alkylpyrrolidone, J. Surfactant Deterg. 25 (1) (2021), https://doi.org/10.1002/jsde.12544.
[36] B. Petkova, S. Tcholakova, Foamability and foam stability of alkyl sarcosinates at different pHs, 2025 in preparation.
[37] W.M. Haynes (Ed.), CRC Handbook of Chemistry and Physics, 94th edition, CRC Press LLC, Boca Raton, FL, 2013–2014.
[38] W.M. Haynes (Ed.), CRC Handbook of Chemistry and Physics, 95th edition, CRC Press LLC, Boca Raton, FL, 2014–2015.
[39] G. Georgieva, S. Anachkov, I. Lieberwirth, K. Koynov, P. Kralchevsky, Synergistic growth of giant wormlike micelles in ternary mixed surfactant solutions: effect of octanoic acid, Langmuir 32 (2016) 12885–12893.
[40] C. Tanford, The hydrophobic effect: formation of micelles and biological membranes, second edition, Wiley, New York, 1980.
[41] J. Kestin, H.E. Khalifa, R.J. Correia, Tables of the dynamic and kinematic viscosity of aqueous NaCl solutions in the temperature range 20–150 °C and the pressure range 0.1–35 MPa, J. Phys. Chem. Ref. Data 10 (1981) 71–88, https://doi.org/10.1063/1.555641.
[42] P. Kralchevsky, K. Danov, C. Pishmanova, S. Kralchevska, N. Christov, K. Ananthapadmanabhan, A. Lips, Effect of the precipitation of neutral-soap, acid-soap, and alkanoic acid crystallites on the bulk pH and surface tension of soap solutions, Langmuir 23 (7) (2007) 3538–3553.
[43] M. Boneva, K. Danov, P. Kralchevsky, S. Kralchevska, K. Ananthapadmanabhan, A. Lips, Coexistence of micelles and crystallites in solutions of potassium myristate: Soft matter vs. solid matter, Colloids Surf. A Physicochem. Eng. Asp. 354 (1–3) (2010) 172–187.
[44] V. Kelleppan, C. Butler, A. Williams, M. Vidallon, L. Giles, J. King, A. Sokolova, L. de Campo, G. Pearson, R. Tabor, K. Tuck, Components of cocamidopropyl betaine: surface activity and self-assembly of pure alkyl amidopropyl betaines, Colloids Surf. A Physicochem. Eng. Asp. 656 (2023) 130435, https://doi.org/10.1016/j.colsurfa.2022.130435.
[45] T. McCoy, J. King, J. Moore, V. Kelleppan, A. Sokolova, L. de Campo, M. Manohar, T. Darwish, R. Tabor, The effects of small molecule organic additives on the self-assembly and rheology of betaine wormlike micellar fluids, J. Colloid Interface Sci. 534 (2019) 518–532, https://doi.org/10.1016/j.jcis.2018.09.046.
[46] P. Hassan, G. Fritz, E. Kaler, Small angle neutron scattering study of sodium dodecyl sulfate micellar growth driven by addition of a hydrotropic salt, J. Colloid Interface Sci. 257 (2003) 154–162.
[47] V. Aswal, P. Goyal, Counterions in the growth of ionic micelles in aqueous electrolyte solutions: a small-angle neutron scattering study, Phys. Rev. E 61 (3) (2000) 2947, https://doi.org/10.1103/PhysRevE.61.2947.